GEOPHYSICAL INVESTIGATIONS AT FLOWERS RANCH, HEMPHILL COUNTY, TEXAS

by

Jeffrey G. Paine and Edward W. Collins

Bureau of Economic Geology
John A. and Katherine G. Jackson School of Geosciences
The University of Texas at Austin
University Station, Box X
Austin, Texas 78713

Corresponding author
jeff.paine@beg.utexas.edu
(512) 471-1260
TBPG License No. 3776

Report Prepared for Intera under Technical Services Agreement UTAUS CN: 8768

October 2011

CONTENTS

FIGURES

TABLE

INTRODUCTION

Intera Inc. requested technical assistance from the Bureau of Economic Geology (BEG) to conduct ground-based geophysical surveys at Flowers Ranch to acquire noninvasive data that would help determine whether there was evidence for contamination of sedimentary strata and groundwater between the base of the Ogallala Formation and the ground surface near the Jones 5-49H well on the Flowers Ranch in Hemphill County, Texas. On May 19-21, 2011, BEG researchers conducted frequency- and time-domain electromagnetic induction (EM) geophysical measurements near the well to identify ground conductivity anomalies that could be associated with the presence of saline water introduced into the shallow subsurface during drilling activities at the site. EM surveys consisted of (1) three ground-conductivity transects (Lines 1, 2, and 3, Fig. 1) in the vicinity of the well, the blowout feature on the bank of the creek east of the well, and along the axis of the creek upstream to measure apparent electrical conductivity of the ground to depths from a few to a few tens of meters, and (2) five time-domain EM soundings on the periphery of the 5-49H well pad (FR2, FR3, FR4, FR5, and FR7, Fig. 1) intended to produce multi-layer conductivity profiles between the ground surface and the base of the Ogallala Formation that could reveal conductivity anomalies that might be indicative of volumetrically significant salinization within the upper 300 m of the subsurface. Dry soil and ground that is partly or completely saturated with fresh water has relatively low electrical conductivity (generally a few to a few tens of milliSiemens per meter [mS/m]; NcNeill, 1980a). Ground that has been salinized through the introduction of highly conductive saline fluids (Hem, 1985) commonly associated with oil and gas drilling and production activities has much higher conductivities ranging from a few tens to a few hundred mS/m. Electrical geophysical methods such as EM and resistivity are thus highly effective in identifying salinized soil and groundwater.

METHODS

Ground conductivity measurements along lines 1, 2, and 3 were acquired using a Geonics EM34-3 ground conductivity meter. This is a frequency-domain EM system that consists of two circu-

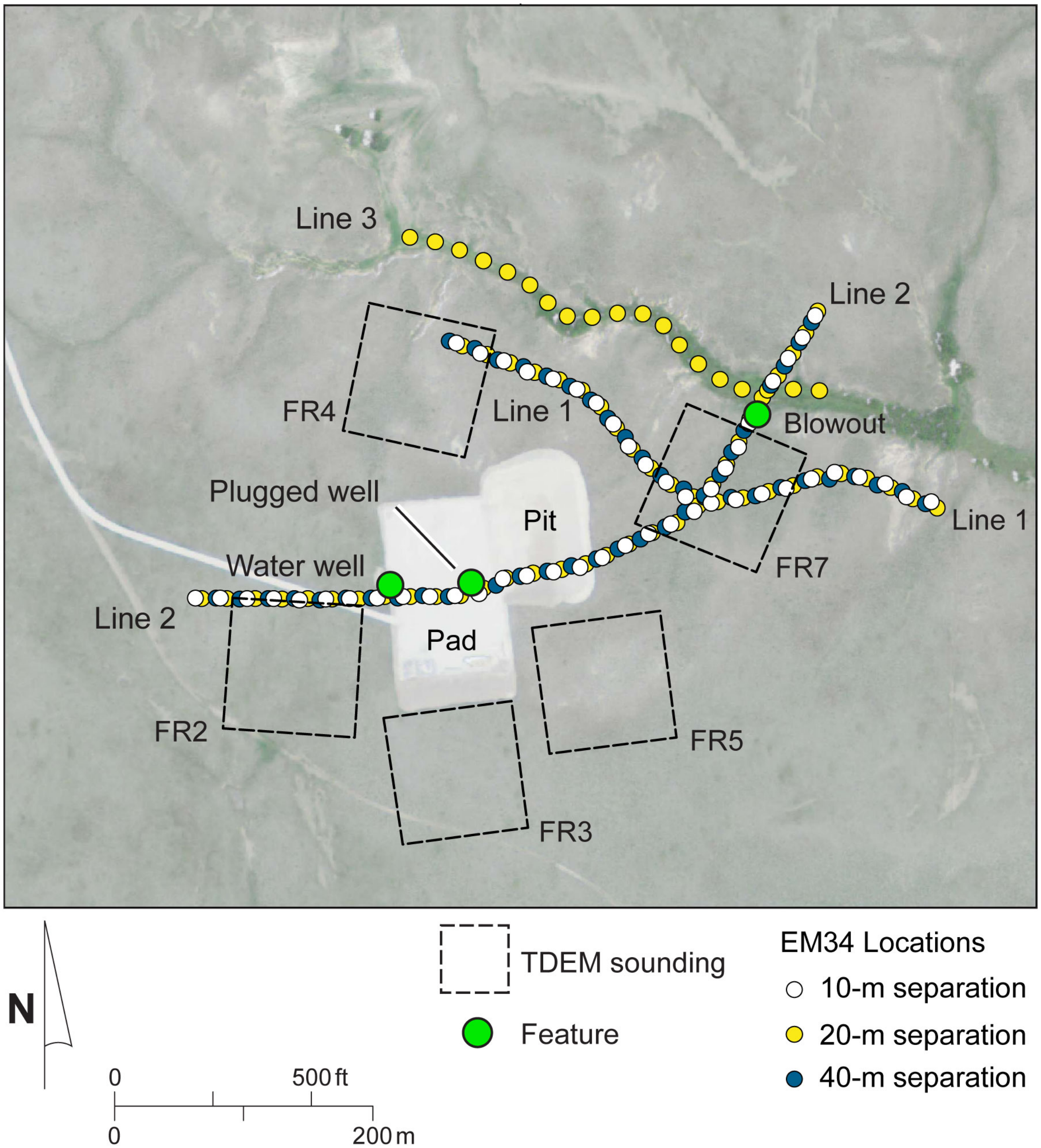

Figure 1. Aerial photographic image of the wellsite area showing the location of apparent ground conductivity measurements using the Geonics EM34-3 (white, yellow, and blue circles) and the time-domain electromagnetic induction soundings (FR2, FR3, FR4, FR5, and FR7, dashed rectanges). The plugged well, water-supply well, and blowout locations are also shown. Photographic image (dated 2010) acquired as part of the National Agriculture Imagery Program courtesy of the Texas Natural Resources Information System.

lar coils (one transmitter and one receiver) that are operated at three fixed, primary frequencies and associated coil separations. At each frequency, a continuously varying current oscillates at the primary frequency through the transmitter coil, creating a continuously varying magnetic field around the coil. Following Faraday's Law of Induction, this continuously varying primary magnetic field induces electrical currents to flow in the ground beneath the coils, in proportion to the electrical conductivity of the ground. These ground currents generate their own magnetic field, which is detected at the receiver coil. The strength of the currents flowing in the ground is proportional to the electrical conductivity of the ground, allowing the instrument to measure ground conductivity by comparing the strength of the primary and secondary magnetic fields. Changes in exploration depth of the instrument are achieved by changing the coil separation and primary frequency (larger separations and lower frequencies explore deeper into the subsurface). At 10-m coil separation and a primary frequency of 6400 Hz, the instrument explores to a maximum depth of about 6 m with the coils aligned in a vertical plane (horizontal dipole, or HD) and about 12 m with the coils lying flat on the ground (vertical dipole, or VD). Similarly, approximate exploration depths increase to about 12 m (HD) and 25 m (VD) at a 20-m coil separation and a primary frequency of 1600 Hz. In its deepest-exploring configuration (40-m coil separation and 400 Hz primary frequency), approximate exploration depths reach about 25 m (HD) and 50 m (VD) (McNeill, 1980b). The instrument records an apparent conductivity value at each coil separation and orientation that represents a value integrated over the exploration depth achieved in that configuration.

Along EM lines 1 and 2, we acquired apparent conductivity measurements at all six available configurations (HD and VD measurements at the three available coil separations, Appendix A), allowing conductivity changes to be depicted laterally along the lines as well as with changes in exploration depth.

Because the exploration depth of the EM34 is limited by signal strength and instrument configuration to a few tens of meters at most, we acquired EM soundings using the time-domain

(TDEM) method (Kaufman and Keller, 1983) to enable exploration to greater than 200-m depth. In the TDEM method as used at Flowers Ranch, a single-wire loop is laid out in a square measuring 100 m on each side. A constant current is applied to the wire, which sets up a static magnetic field around the transmitter loop. The current is abruptly terminated, which causes the magnetic field to collapse. This collapsing field induces currents to flow in the ground that propagate downward with time. These ground currents generate a secondary magnetic field that induces current to flow in the receiver loop, which in our case is the same loop of wire that served as the transmitter. The reciever (terraTEM instrument manufactured by Monex GeoScope Ltd.) measures the strength and decay of the secondary magnetic field over a few to a few tens of milliseconds after the transmitter current is turned off. In general, the shape of the decay is controlled by the conductivity structure of the ground. At early times after current shutoff, the measured field is influenced strongly by the conductivity of shallow strata. At later times, after currents have been induced at successively greater depths, the measured field is progressively more influenced by electrical conductivity of the ground at greater depths. Maximum exploration depth increases with loop size, loop current, and recording time. Background EM noise from power lines, electrical storms, and other sources limits the exploration depth that can be achieved in a given instrument configuration.

Commercial software (IX1D by Interpex Limited) is used to determine the subsurface conductivity changes with depth that would produce a decay that best fits the actual observed decay (Appendix B).

FREQUENCY-DOMAIN EM SURVEY

EM lines 1, 2, and 3 were placed to determine the lateral extent of conductive ground within the upper few tens of meters around the well pad, pit, blowout feature, and the adjacent creek (Fig. 1). Apparent ground conductivities were measured in the HD and VD coil orientations at 174 locations (Table 1, Appendix A), including 66 locations along line 1 on the slope adjacent to the pit, 89 locations along line 2 extending from west of the well pad and water well, adjacent to

Table 1. Statistical summary of EM34-3 ground conductivity measurements along lines 1, 2, and 3 at Flowers Ranch (Fig. 1).

	n	Minimum (mS/m)	Maximum (mS/m)	Average (mS/m)	Std. Dev. (mS/m)
All 10 HD	52	11	91	28.6	16.1
All 10 VD	52	13	130	38.4	21.7
All 20 HD	71	22	91	47.8	17.4
All 20 VD	71	7	270	54.1	34.1
All 40 HD	51	37	96	56.8	16.1
All 40 VD	51	18	84	43.8	13.3
Line 1, 10 HD	22	17	56	27.3	9.2
Line 1, 10 VD	22	23	58	34.7	10.2
Line 1, 20 HD	22	32	78	42.5	11.9
Line 1, 20 VD	22	34	70	45.3	8.4
Line 1, 40 HD	22	43	75	51.8	8.0
Line 1, 40 VD	22	18	68	45.1	10.3
Line 2, 10 HD	30	11	91	29.6	19.7
Line 2, 10 VD	30	13	130	41.1	26.9
Line 2, 20 HD	30	22	91	47.1	23.1
Line 2, 20 VD	30	7	131	49.2	23.9
Line 2, 40 HD	29	37	96	60.6	19.2
Line 2, 40 VD	29	20	84	42.8	15.0
Line 3, 20 HD	19	47	71	55.1	5.9
Line 3, 20 VD	19	45	270	72.2	53.8

the blowout feature, and across the creek, and 19 locations (at 20-m coil separation only) along the creek axis from a point about 320 m upstream from the blowout feature to about 40 m downstream from it.

Line 1

Line 1 roughly parallels the creek and extends along the slope between the well pad and pit area and the creek. It was intended to intersect potential shallow subsurface pathways between the well area and the blowout feature, extending from likely background areas at the northwest end of the line.

Along this line, average conductivities are higher at the deeper-exploring 20- and 40-m coil separations (42 to 52 mS/m, Table 1) than at the shallower-exploring 10-m coil separation (27 to 35 mS/m). At each coil separation and orientation, apparent conductivities are highest in the central part of the line between the southern edge of the pit and the blowout feature. Background conductivities at the northwestern part of the line are below 30 to 36 mS/m for the 10-m HD and VD orientations, below 36 to 42 mS/m for the 20-m HD and VD orientations, and below 49 to 58 mS/m for the 40-m HD and VD orientations (Figs. 2 to 7).

At each separation and orientation except the deepest exploring (40-m VD), apparent conductivites increase in the central part of the line to the highest ranges observed (43 to 60 mS/m for the 10-m HD and VD orientations, 43 to 62 mS/m for the 20-m HD and VD orientations, and 50 to 84 mS/m for the 40-m HD orientation). Average apparent conductivities measured with the 40-m VD orientation drop below those observed for the shallower-exploring 40-m HD orientation (from 51.8 to 45.1 mS/m, Table 1). There is no obvious high at this orientation in the central part of the line. This observation suggests that the anomalously high apparent conductivities measured in the shallower-exploring orientations do not extend to the greater depths reached by the 40-VD orientation.

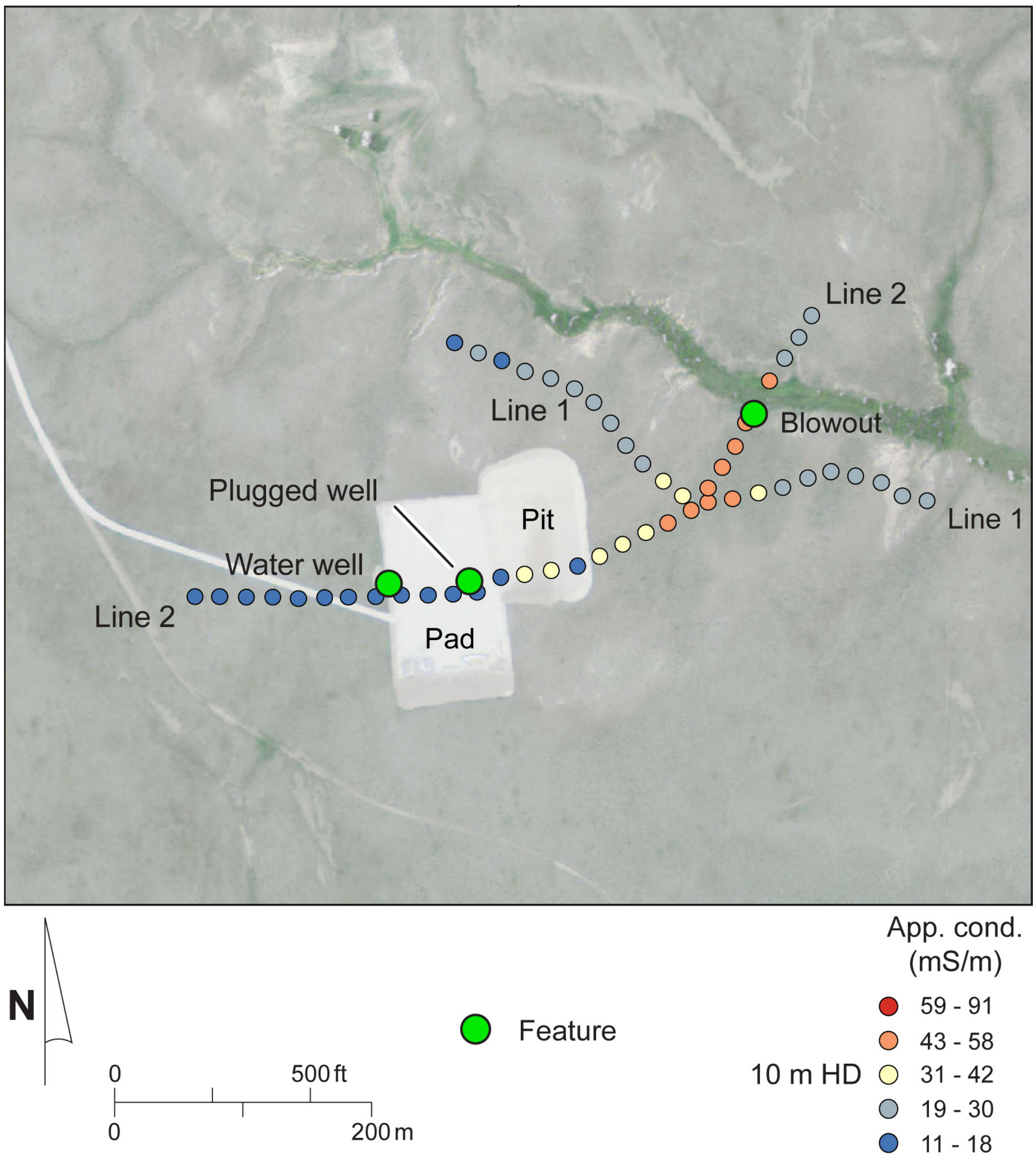

Figure 2. Apparent ground conductivity measured using the Geonics EM34-3 instrument at 10-m coil separation and horizontal dipole coil orientation. In this configuration, the instrument responds most strongly to material between the surface and a depth of about 6 m.

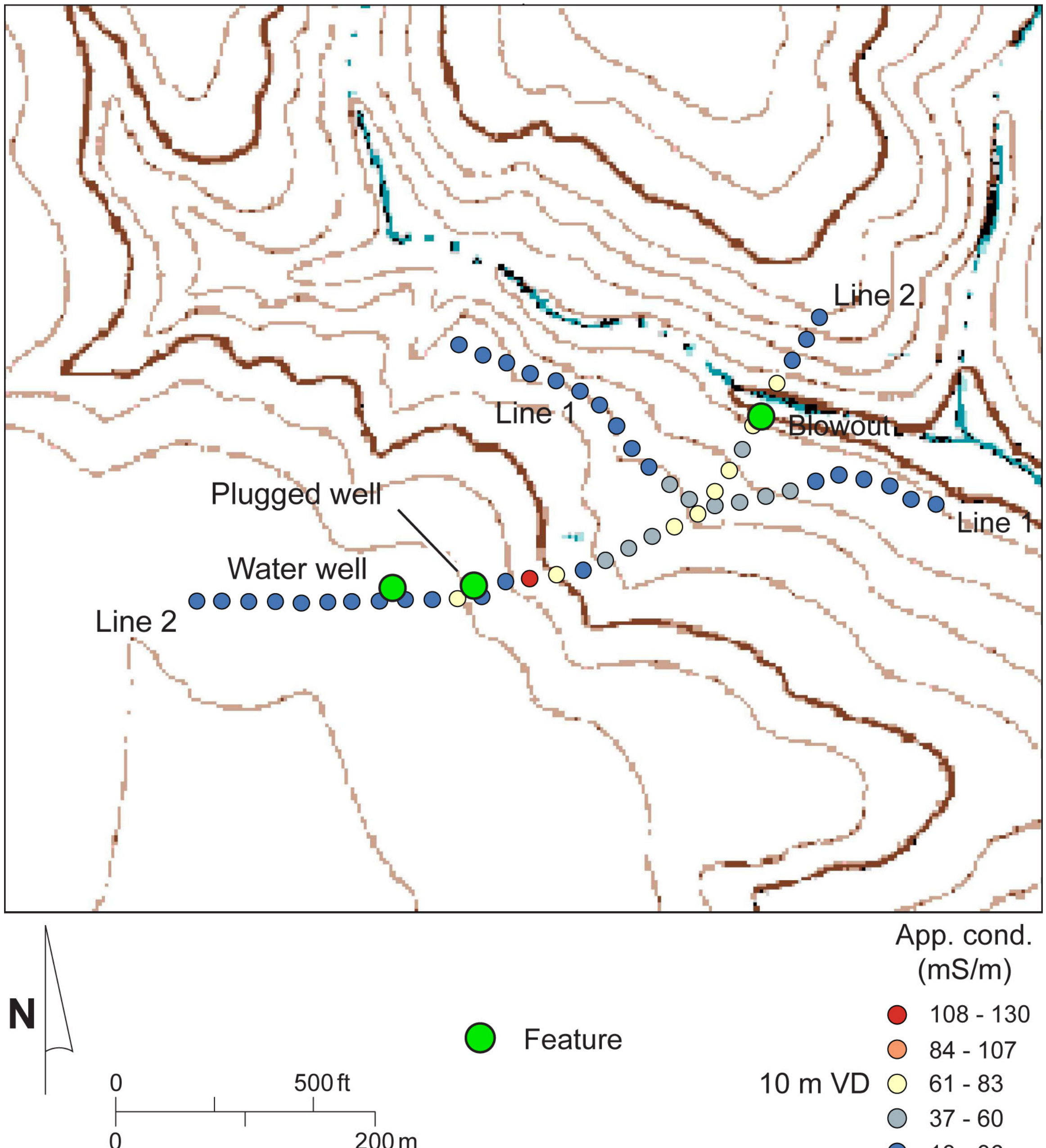

Figure 3. Apparent ground conductivity measured using the Geonics EM34-3 instrument at 10-m coil separation and vertical dipole coil orientation. In this configuration, the instrument responds most strongly to material between the surface and a depth of about 12 m. Data are superimposed on a 1967 U.S.G.S. topographic map of the Canadian SE quadrangle scanned by the Texas Natural Resource Information System.

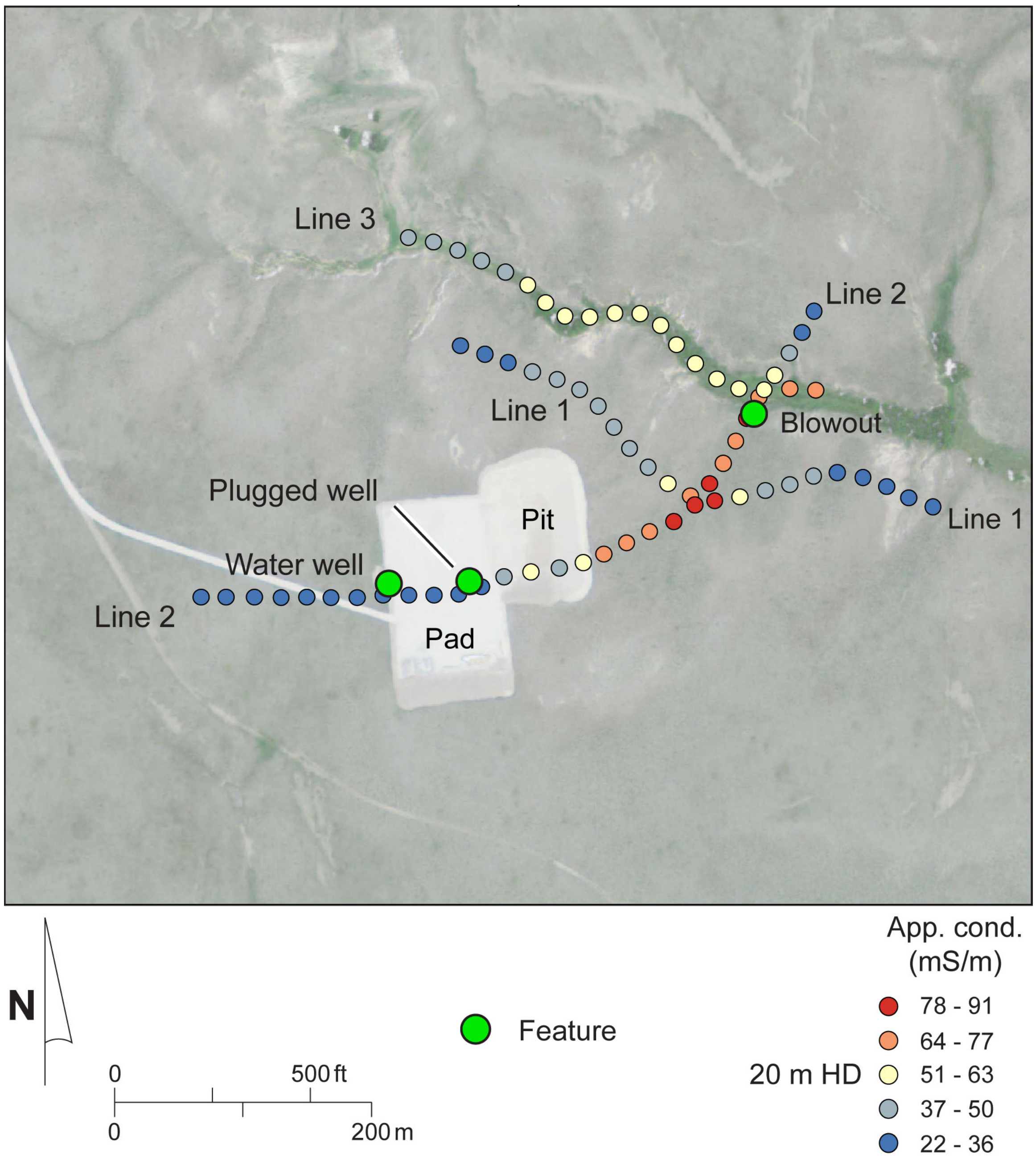

Figure 4. Apparent ground conductivity measured using the Geonics EM34-3 instrument at 20-m coil separation and horizontal dipole coil orientation. In this configuration, the instrument responds most strongly to material between the surface and a depth of about 12 m.

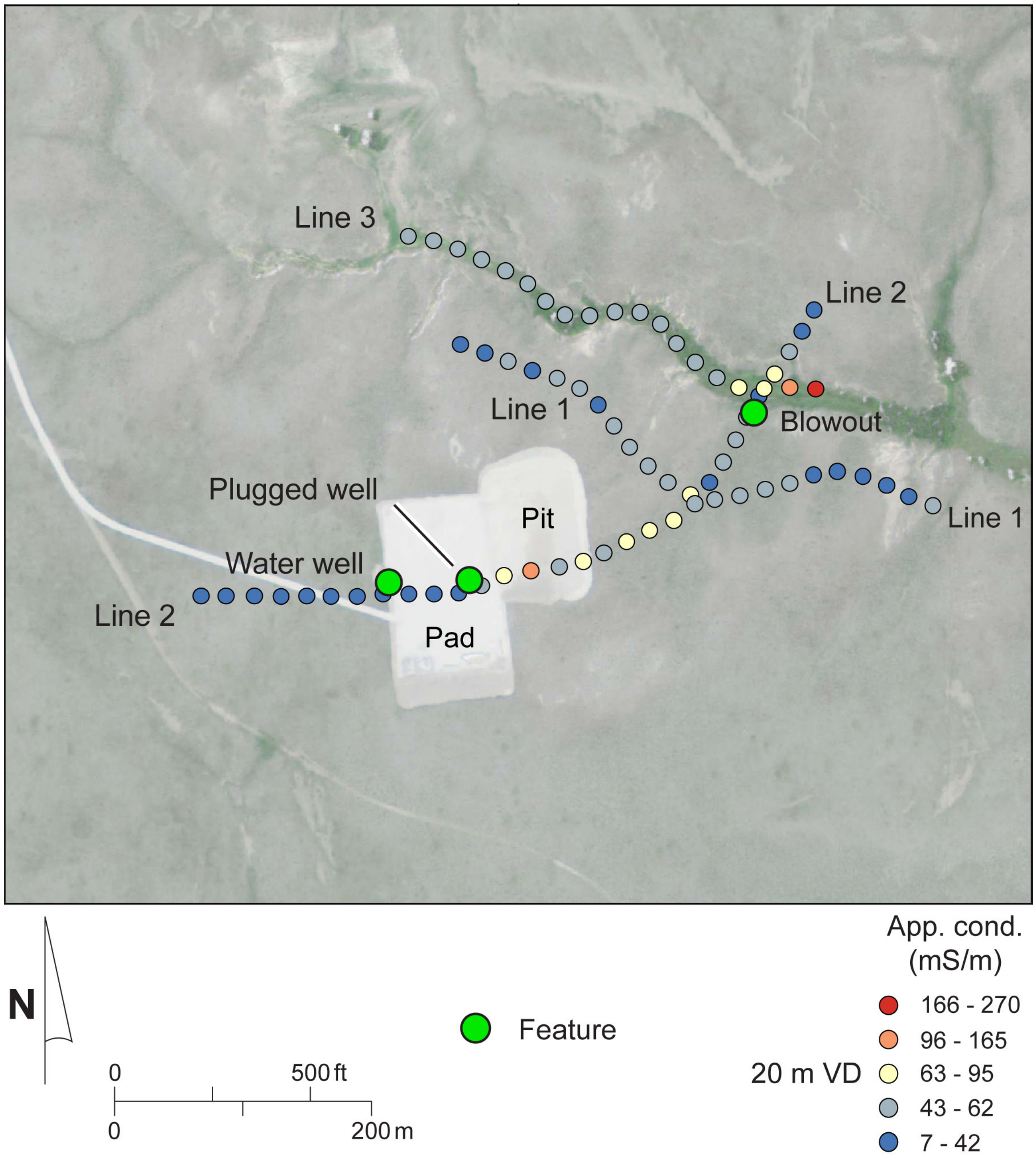

Figure 5. Apparent ground conductivity measured using the Geonics EM34-3 instrument at 20-m coil separation and vertical dipole coil orientation. In this configuration, the instrument responds most strongly to material between the surface and a depth of about 24 m.

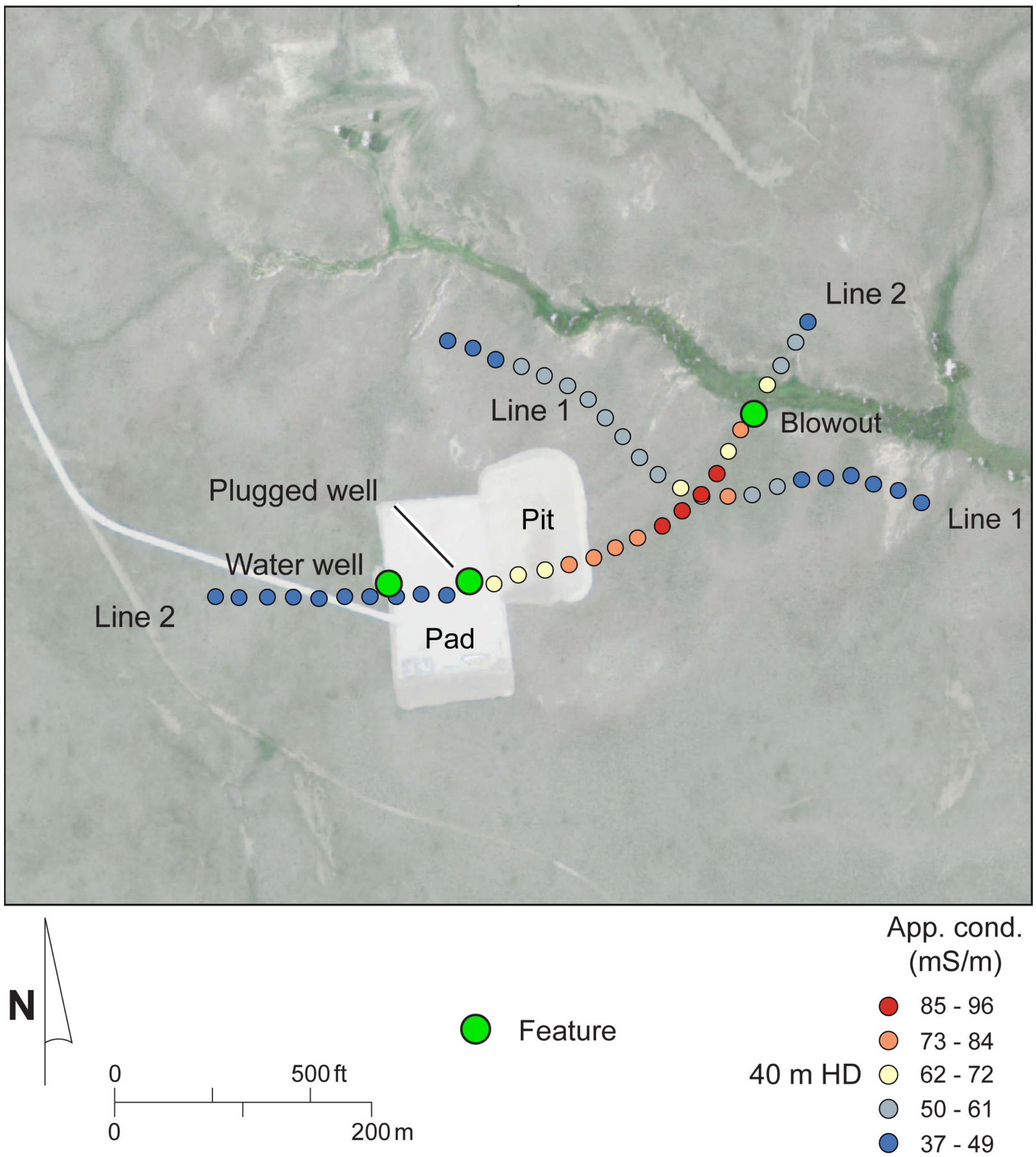

Figure 6. Apparent ground conductivity measured using the Geonics EM34-3 instrument at 40-m coil separation and horizontal dipole coil orientation. In this configuration, the instrument responds most strongly to material between the surface and a depth of about 24 m.

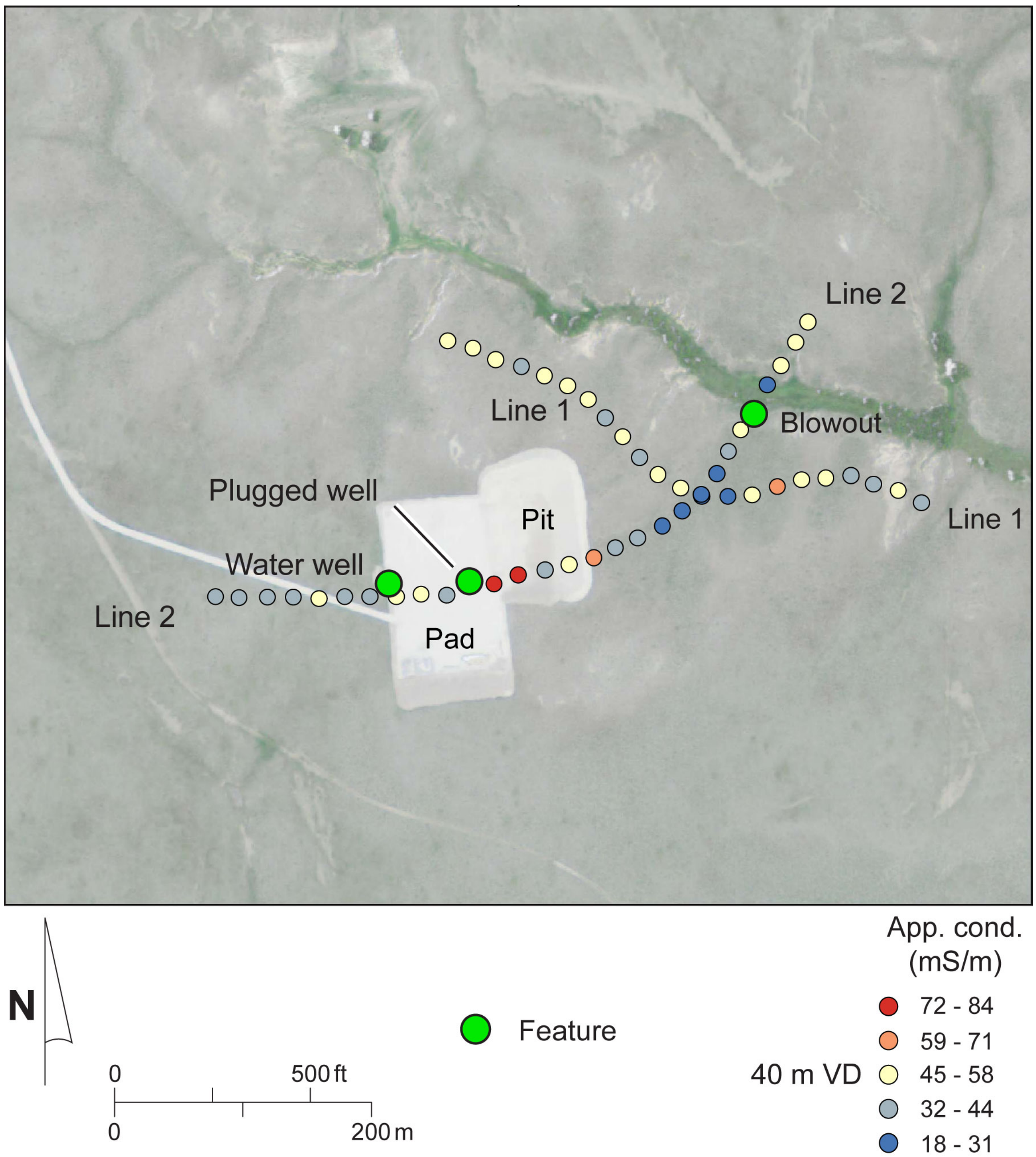

Figure 7. Apparent ground conductivity measured using the Geonics EM34-3 instrument at 40-m coil separation and vertical dipole coil orientation. In this configuration, the instrument responds most strongly to material between the surface and a depth of about 50 m.

Apparent conductivities recorded in each of the coil separations and orientations can be assigned an apparent depth, gridded, and viewed as a pseudosection that depicts lateral extent of elevated conductivity at multiple coil orientations (and apparent depths) simultaneously (Fig. 8). By calculating apparent depths as 10 percent of the coil separation for the shallow-weighted HD orientation and 60 percent of the coil separation in the center-weighted VD orientation, a qualitative depiction of the results shows that elevated apparent conductivities are highest in the shallow subsurface (upper 10 m or so) within an approximately 120-m wide zone in the surface spill area adjacent to the southeast part of the pit (Fig. 8a).

Line 2

Line 2 is about 600-m long (Fig. 1), extending from a presumed background area more than 200 m west of the 5-49H well, eastward across the well pad and adjacent to the water well and 5-49H well, across the southern floor of the pit, along the axis of the spill area, and then northeastward adjacent to the blowout feature, across the creek, and up the slope on the northeast side of the creek.

Average apparent conductivities are higher at every coil separation and orientation along line 2 than they are along line 1 (Table 1). Average apparent conductivities increase with increasing exploration depth from a low of 29.6 mS/m in the shallowest-exploring, 10-m HD orientation to a high of 60.6 mS/m in the 40-m HD orientation, but then fall to 42.8 mS/m at the deepest-exploring, 40-m VD orientation. This suggests that the shallow elevated conductivities measured along this line are generally shallower than the maximum exploration depth of the EM34 instrument.

The lowest apparent conductivities along this line were measured west of the pad (Figs. 2 to 7). The lowest values were observed in this area at all but the 40-m VD orientation (11 to 36 mS/m at the 10-m HD and VD orientations, 22 to 42 mS/m at the 20-m HD and VD orientations, and 37 to 49 mS/m at the 40-m HD orientation). Locally high values were measured on the pad in the 40-m VD orientation (Fig. 7) that are an effect of the presence of highly conductive metal (well

(a)

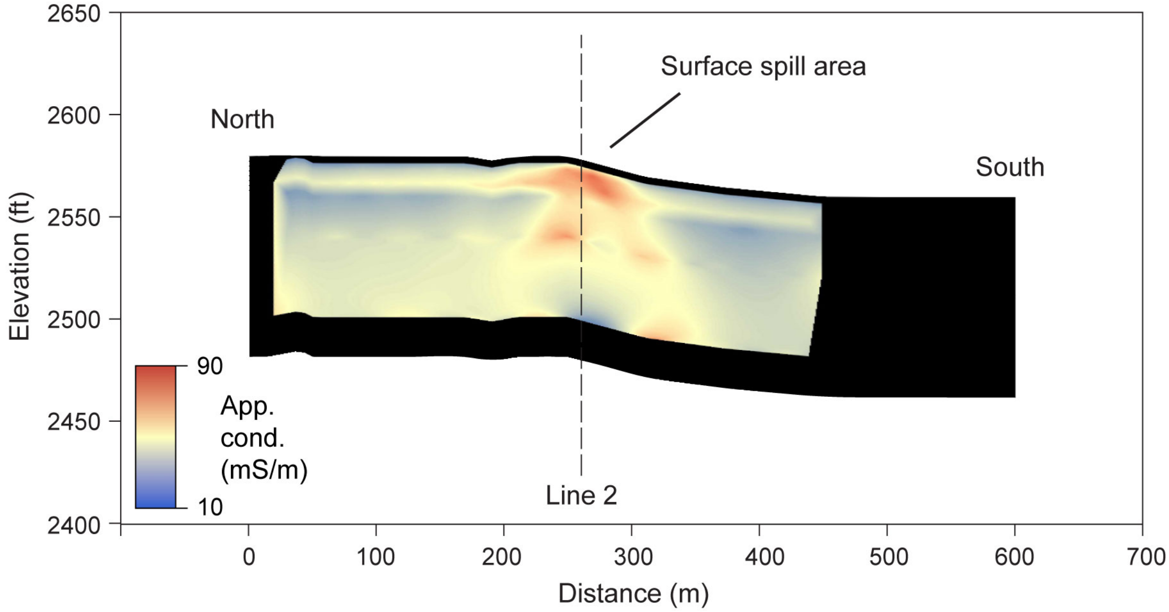

(a)

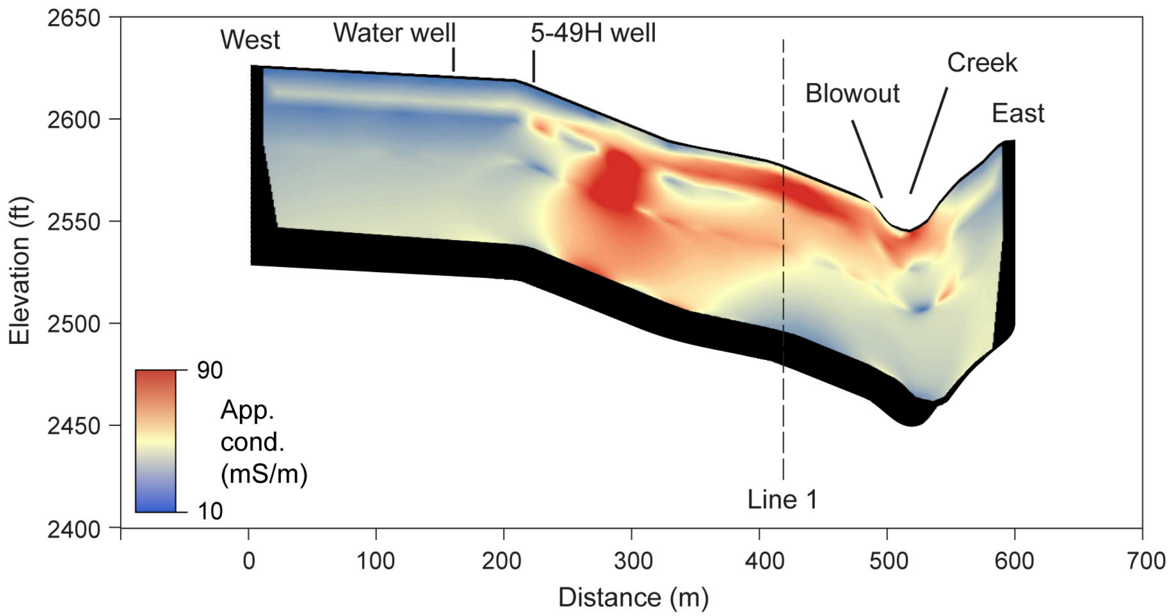

Figure 8. Apparent conductivity pseudosections along (a) line 1 and (b) line 2 constructed by gridding apparent conductivity values for 10-, 20-, and 40-m coil separations and assuming apparent depths for each measurement at 10 percent of the coil spacing for HD measurements and 60 percent of the coil spacing for VD measurements.

casing and pipe) at and near the surface. Highest apparent conductivities at the other coil orientations are measured between the pit and the blowout feature (43 to 96 mS/m at the 10-m HD and VD orientations, 64 to 95 mS/m at the 20-m HD and VD orientations, and 73 to 96 mS/m at the 40-m HD orientation). At each orientation except the 40-m VD, apparent conductivities are two or more times higher in the nearly 200-m long segment from the pit to the blowout feature and adjacent creek than they are in the presumed background area west of the well pad.

The line 2 pseudosection (Fig. 8b), constructed as a visualization aid from all apparent conductivities and apparent depths estimated as 10 percent of the HD coil spacing and 60 percent of the VD coil spacing, depicts low, background apparent conductivities west of the 5-49H well and elevated apparent conductivities that extend eastward from the pit area to the blowout feature and creek bed.

Line 3

Apparent conductivity measurements were acquired at the 20-m coil spacing along the creek axis for a total distance of about 360 m, including about 320 m upstream from the blowout feature (Fig. 1). Measurements along this line were intended to determine the background ground conductivity upstream from the blowout feature as well as the upstream limit of elevated ground conductivity near the blowout feature.

Average apparent conductivities at the 20-m separation were higher along this line (55.1 mS/m at the 20-m HD orientation and 72.2 mS/m at the 20-m VD orientation, Table 1) than they were at the same orientation along lines 1 and 2. In the HD orientation, lowest apparent conductivities (between 37 and 50 mS/m, Fig. 4) were measured along a 80- to 100-m long segment at the upstream end of the line. Apparent conductivities increased to 51 to 63 mS/m along the 220-m long creekbed segment downstream to the blowout feature, at which point the measured apparent conductivities increased to the 64 to 77 mS/m range. In the deeper-exploring 20-m VD orientation (Fig. 5), apparent conductivities upstream from the blowout feature were in the 43 to 62 mS/m range, increasing to the highest apparent conductivities observed at the site (63 to 270 mS/m) near the blowout feature.

TIME-DOMAIN EM SURVEY

Five TDEM soundings were acquired around the periphery of the 5-49H well pad and pit (Fig. 1) to determine the generalized conductivity structure through the Ogallala aquifer to depths greater than the tens of meters achievable with the EM34. Lack of significant EM noise sources (power lines, electrical storms, and metallic debris) allowed TDEM decays to be observed beyond 10 milliseconds at the site, which achieved exploration depths through the Ogallala and into conductive, pre-Ogallala strata at each of the five sites. Multiple recordings were made at each site with differing acquisition parameters to examine response variability. Processing consisted of selecting the best decays at each site, and then proceeding through one- to five-layer models to identify the conductivity models that would yield the best fits to the observed decays. Four of the soundings (FR2, FR3, FR4, and FR5, Figs. 1 and 9 to 13, Appendix B) required five-layer models to produce acceptably low fitting errors of 1.2 to 1.8 percent. Sounding FR7, located between the pit and the blowout feature, required four layers to achieve a 1.3 percent fitting error.

Noninvasive TDEM soundings yield generalized conductivity profiles of the subsurface that do not have the vertical resolution that could be achieved using borehole geophysical tools. Major features evident in the soundings include a basal conductive layer (188 to 395 mS/m, Appendix B) at depths greater than 243 to 275 m, which likely represents conductive Permian or Triassic strata beneath the Ogallala, and three or four layers of less conductive strata within the Ogallala and younger strata. At four of the soundings, located north, south, and west of the well pad and pit (FR2, FR3, FR4, and FR5, Fig. 1), a moderately conductive zone (layer 2) occurs at depths modeled at 8 to 40 m (FR2), 24 to 47 m (FR3), 24 to 41 m (FR4), and 18 to 36 m (FR5) (Figs. 9 to 12, Appendix B). This layer, which underlies a poorly conductive surface layer that likely represents unsaturated surficial strata, is interpreted to represent increased water or clay content possibly associated with a perching horizon above the main Ogallala aquifer. Below this

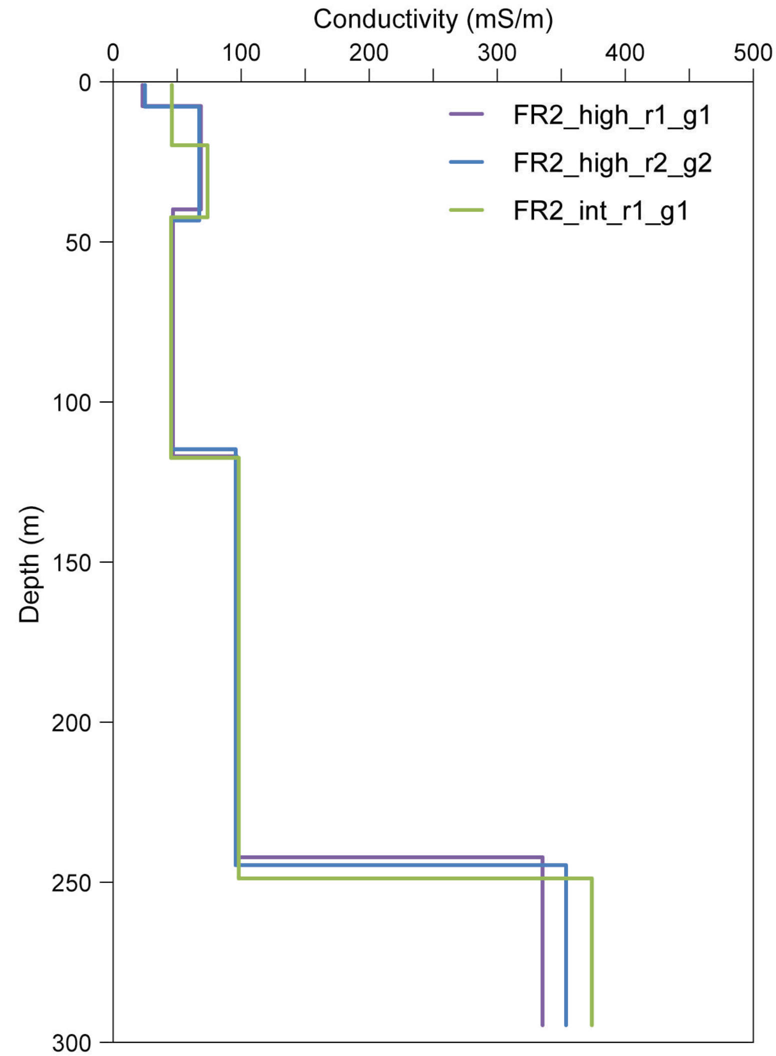

Figure 9. Ground conductivity profile models that fit the time-domain decay observed at TDEM site FR2 (Fig. 1).

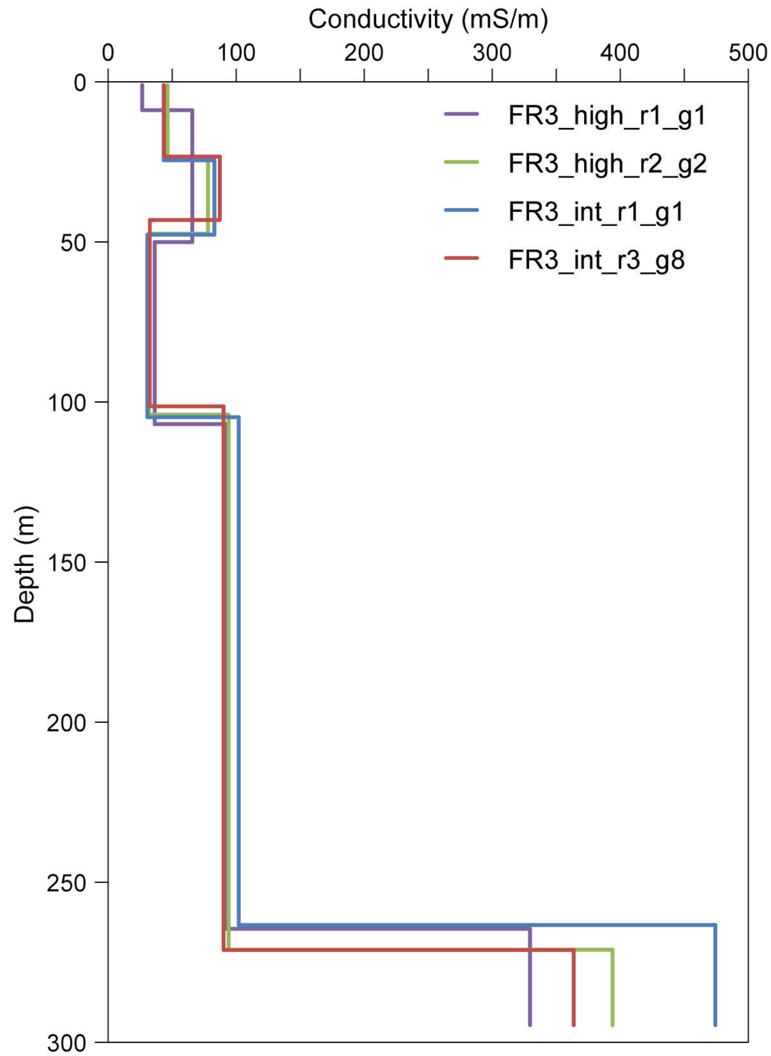

Figure 10. Ground conductivity profile models that fit the time-domain decay observed at TDEM site FR3 (Fig. 1).

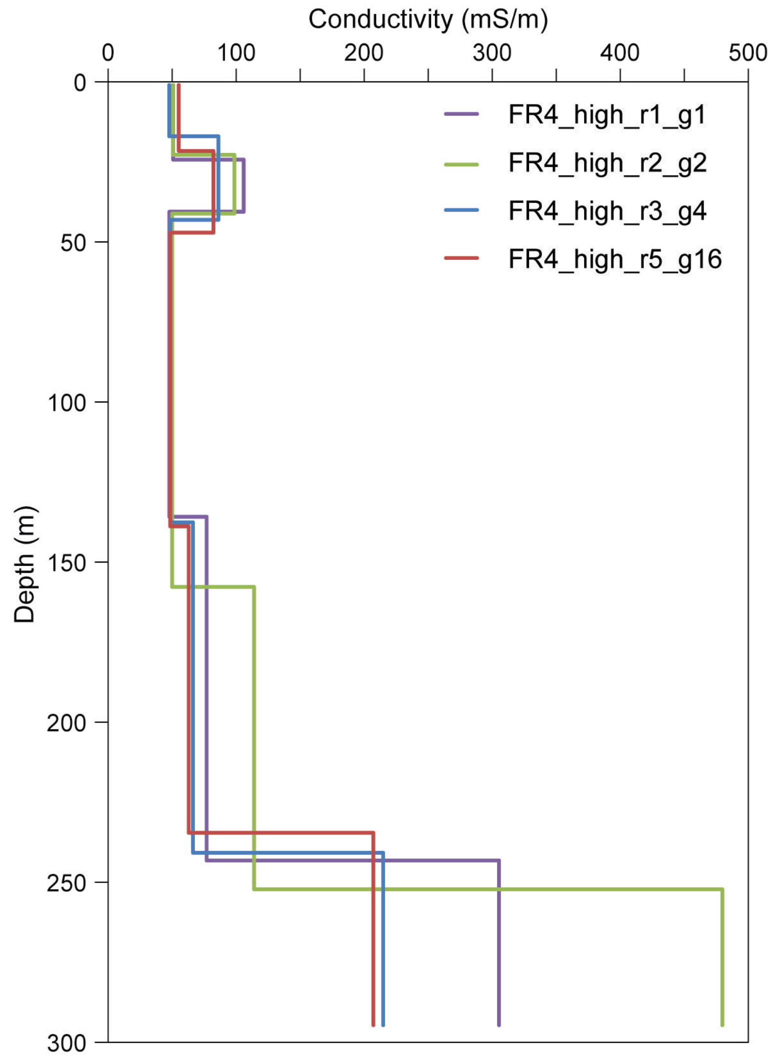

Figure 11. Ground conductivity profile models that fit the time-domain decay observed at TDEM site FR4 (Fig. 1).

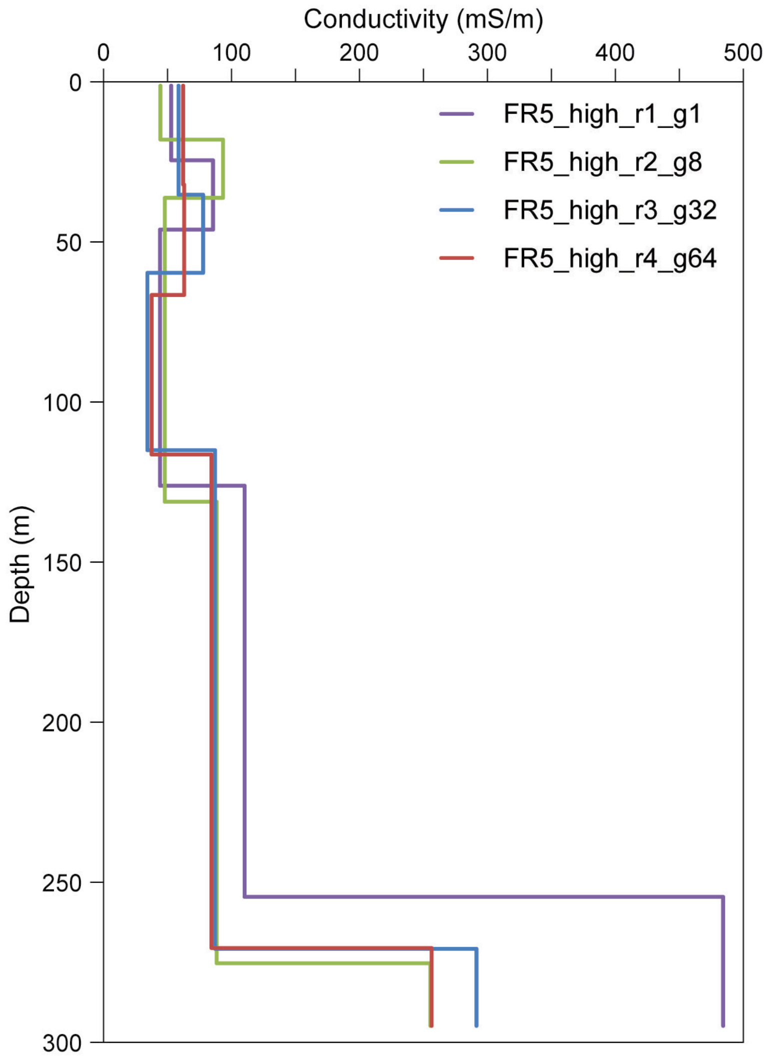

Figure 12. Ground conductivity profile models that fit the time-domain decay observed at TDEM site FR5 (Fig. 1).

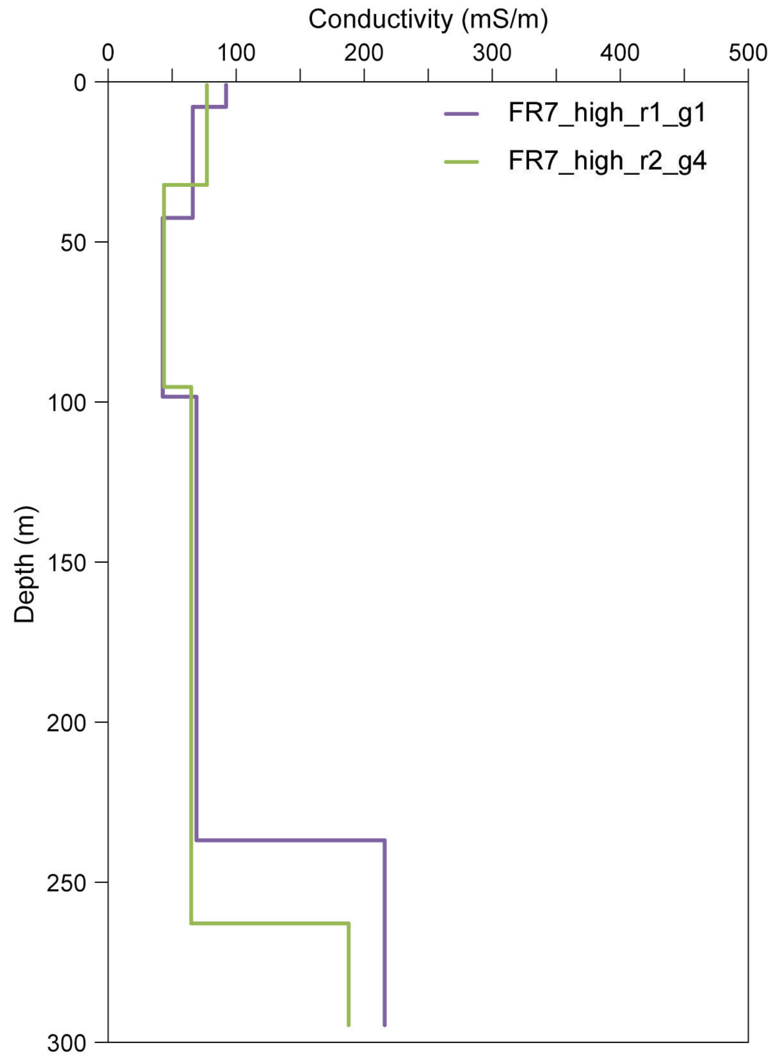

Figure 13. Ground conductivity profile models that fit the time-domain decay observed at TDEM site FR7 (Fig. 1).

layer, lower conductivities (layer 3) are encountered to depths ranging from about 104 to 131 m, where conductivities increase to 77 to 97 mS/m within layer 4 and continue downward until the basal conductive layer is reached. In these four soundings, layer 4 is interpreted to represent the main Ogallala aquifer. Similar depths, conductivities, and stratal interpretations apply to sounding FR7 (Fig. 13, Appendix B), except that there is no poorly conductive surface layer at this site. A conductive layer is present at the surface, coinciding with the shallower conductive zone identified along EM lines 1 and 2 between the pit and the blowout feature.

CONCLUSIONS

Noninvasive EM transects and soundings acquired at Flowers Ranch delimited the extent of background and elevated ground conductivity in the shallow subsurface near the 5-49H well that could be associated with drilling-related saline fluid invasion. Within the upper 20 to 30 m, elevated ground conductivities were measured between the pit and blowout feature adjacent to the creek, and along the creek near the blowout feature. A sounding in the elevated conductivity area between the pit and the blowout feature also detected elevated conductivities from the surface to depths of 10 to 30 m. Deep soundings reached beyond the base of the Ogallala, detecting layers interpreted to represent an unsaturated near-surface layer, an Ogallala perching layer with elevated clay or water content, the saturated main Ogallala aquifer, and a basal, pre-Ogallala conductive layer.

ACKNOWLEDGMENTS

This work was conducted under Technical Services Agreement UTAUS CN: 8768 between Intera Inc. and The University of Texas at Austin, Bureau of Economic Geology. Jeffrey G. Paine served as principal investigator. Van Kelley and Joe Galemore (Intera) served as project managers and assisted with field activities. The authors gratefully acknowledge access and field support from the landowners Kim and Kirk Flowers.

REFERENCES

Hem, J. D., 1985, Study and interpretation of the chemical characteristics of natural water: U.S. Geol. Survey, Professional Paper 2254, 263 p.

McNeill, J. D., 1980a, Electrical conductivity of soils and rocks: Geonics Ltd., Mississauga, Ont., Technical Note TN-5, 22 p.

McNeill, J. D., 1980b, Electromagnetic terrain conductivity measurement at low induction numbers: , Geonics Ltd., Mississauga, Ont., Technical Note TN-6, 15 p.

Spies, B. R., and Frischknecht, F. C., 1991, Electromagnetic sounding, in Electromagnetic Methods: *in* Nabighian, M. N., editor, Applied Geophysics—Applications, Part A and Part B: Society of Exploration Geophysicists, Tulsa, p. 285–386.

APPENDIX A: FREQUENCY-DOMAIN EM MEASUREMENTS

Apparent ground conductivity measurements acquired at the Flowers Ranch site (Fig. 1) using the Geonics EM34-3 ground conductivity meter. Center point location, transmitter and receiver coil separation, and apparent conductivity measurement in the horizontal (HD) and vertical (VD) dipole coil orientation are given. Center point location is calculated as the point midway between the transmitter and receiver locations, which were established using a hand-held GPS unit. Easting and Northing coordinates are in the Universal Transverse Mercator projection, zone 14 north, World Geodetic System 1984 datum, in meters.

Line	Distance along line (m)	Easting (m)	Northing (m)	Coil separation (m)	Apparent conductivity (HD, mS/m)	Apparent conductivity (VD, mS/m)
1	30	385450.5	3960437.8	10	17	23
1	50	385469.0	3960429.5	10	19	25
1	70	385487.5	3960424.0	10	18	28
1	90	385505.5	3960415.5	10	23	26
1	110	385525.5	3960410.0	10	21	30
1	130	385544.0	3960402.0	10	23	28
1	150	385559.0	3960391.0	10	25	30
1	170	385572.0	3960375.0	10	23	36
1	190	385584.0	3960357.5	10	28	36
1	210	385597.0	3960343.5	10	30	34
1	230	385613.0	3960330.0	10	32	41
1	250	385628.0	3960318.5	10	40	58
1	270	385648.0	3960313.5	10	56	51
1	290	385667.0	3960316.0	10	47	57
1	310	385687.0	3960320.5	10	31	50
1	330	385706.0	3960325.0	10	25	37
1	350	385725.5	3960332.5	10	26	30
1	370	385743.5	3960337.5	10	24	28
1	390	385763.0	3960334.0	10	23	24
1	410	385782.5	3960328.5	10	23	29
1	430	385799.0	3960318.5	10	24	31
1	450	385818.5	3960314.5	10	22	32
1	30	385455.0	3960435.5	20	32	38
1	50	385474.0	3960429.0	20	34	40
1	70	385492.5	3960422.5	20	35	45
1	90	385511.0	3960415.0	20	37	39
1	110	385530.5	3960409.0	20	37	43

1	130	385548.0	3960401.0	20	39	44
1	150	385562.5	3960388.5	20	40	40
1	170	385574.5	3960372.0	20	39	48
1	190	385587.0	3960355.5	20	44	48
1	210	385601.5	3960341.0	20	47	44
1	230	385616.5	3960328.0	20	52	58
1	250	385634.0	3960318.5	20	68	70
1	270	385653.0	3960314.5	20	78	46
1	290	385672.5	3960317.5	20	61	49
1	310	385692.5	3960322.5	20	45	59
1	330	385711.5	3960327.0	20	39	53
1	350	385730.0	3960334.0	20	37	38
1	370	385748.5	3960336.5	20	35	39
1	390	385768.5	3960333.0	20	33	34
1	410	385787.0	3960325.5	20	33	37
1	430	385804.0	3960317.0	20	35	37
1	450	385823.0	3960310.0	20	34	47
1	20	385445.0	3960439.0	40	48	55
1	40	385465.0	3960433.5	40	47	46
1	60	385482.5	3960424.5	40	47	45
1	80	385502.5	3960419.5	40	49	43
1	100	385520.5	3960412.0	40	50	45
1	120	385538.5	3960404.0	40	50	52
1	140	385554.5	3960393.5	40	50	49
1	160	385568.0	3960379.5	40	51	42
1	180	385581.5	3960364.5	40	53	50
1	200	385594.5	3960348.5	40	55	41
1	220	385609.0	3960335.0	40	60	55
1	240	385626.5	3960324.5	40	65	51
1	260	385643.0	3960318.0	40	64	18
1	280	385663.5	3960318.0	40	75	22
1	300	385682.0	3960319.0	40	58	48
1	320	385702.0	3960325.5	40	52	68
1	340	385720.5	3960331.0	40	47	52
1	360	385739.5	3960332.5	40	45	49
1	380	385759.0	3960334.5	40	44	43
1	400	385776.5	3960327.5	40	43	36
1	420	385796.0	3960322.5	40	43	45
1	440	385814.0	3960313.0	40	43	38

2	10	385248.5	3960240.0	10	11	16
2	30	385267.5	3960240.0	10	13	16
2	50	385288.5	3960239.5	10	13	14
2	70	385309.0	3960239.5	10	11	17
2	90	385329.0	3960238.5	10	11	18
2	110	385349.5	3960239.0	10	14	13
2	130	385368.0	3960239.5	10	11	17
2	150	385389.0	3960240.0	10	12	16
2	170	385409.5	3960241.0	10	13	16
2	190	385430.0	3960241.0	10	13	17
2	210	385449.5	3960242.0	10	12	75
2	230	385468.0	3960243.5	10	14	32
2	250	385486.5	3960255.0	10	14	33
2	270	385505.0	3960257.5	10	42	130
2	290	385526.0	3960260.5	10	38	82
2	310	385546.5	3960264.0	10	18	26
2	330	385563.5	3960271.5	10	33	45
2	350	385581.5	3960280.5	10	39	41
2	370	385599.5	3960290.0	10	41	48
2	390	385616.5	3960297.5	10	49	60
2	410	385635.0	3960307.5	10	58	69
2	430	385648.0	3960324.5	10	53	64
2	450	385659.0	3960341.0	10	51	71
2	470	385669.0	3960357.0	10	51	54
2	490	385677.0	3960375.5	10	45	66
2	500	385681.0	3960384.5	10	91	32
2	530	385696.0	3960408.0	10	49	60
2	550	385707.5	3960426.0	10	26	33
2	570	385718.5	3960442.0	10	22	28
2	590	385728.5	3960459.0	10	21	25
2	10	385253.0	3960239.5	20	23	29
2	30	385272.5	3960239.5	20	23	32
2	50	385294.5	3960239.5	20	23	32
2	70	385315.5	3960239.0	20	22	32
2	90	385335.5	3960239.5	20	23	35
2	110	385354.5	3960239.0	20	24	30
2	130	385374.5	3960239.0	20	23	34
2	150	385395.0	3960241.0	20	24	33
2	170	385415.0	3960241.0	20	25	36

2	190	385434.5	3960241.0	20	27	41
2	210	385454.0	3960242.0	20	27	14
2	230	385471.5	3960247.5	20	30	57
2	250	385489.0	3960255.5	20	44	91
2	270	385510.0	3960259.5	20	51	131
2	290	385532.0	3960262.5	20	46	52
2	310	385550.5	3960266.5	20	53	78
2	330	385566.5	3960273.0	20	65	62
2	350	385584.5	3960282.0	20	71	71
2	370	385602.5	3960290.5	20	77	66
2	390	385621.0	3960298.5	20	88	68
2	410	385637.5	3960311.5	20	91	52
2	430	385649.0	3960328.0	20	80	41
2	450	385659.5	3960344.0	20	73	58
2	470	385669.5	3960361.0	20	65	44
2	490	385678.0	3960379.0	20	81	54
2	510	385687.5	3960395.5	20	73	7
2	530	385699.5	3960412.5	20	55	71
2	550	385711.0	3960429.5	20	39	43
2	570	385721.0	3960445.5	20	34	39
2	590	385730.5	3960462.5	20	33	42
2	20	385264.5	3960240.0	40	37	39
2	40	385283.0	3960239.0	40	37	42
2	60	385305.0	3960239.5	40	37	40
2	80	385325.0	3960239.5	40	38	42
2	100	385345.0	3960238.5	40	39	45
2	120	385365.0	3960240.0	40	39	41
2	140	385384.5	3960240.0	40	39	44
2	160	385405.0	3960240.0	40	42	48
2	180	385424.5	3960242.0	40	46	49
2	200	385444.5	3960241.0	40	46	32
2	220	385461.5	3960247.5	40	52	44
2	240	385481.5	3960250.0	40	65	80
2	260	385500.0	3960257.0	40	62	84
2	280	385521.0	3960261.0	40	67	40
2	300	385539.5	3960265.0	40	73	51
2	320	385559.0	3960270.5	40	80	69
2	340	385576.0	3960278.0	40	83	41
2	360	385593.0	3960285.5	40	82	42

2	380	385612.5	3960295.0	40	89	24
2	400	385627.5	3960307.0	40	93	24
2	420	385642.5	3960319.5	40	96	20
2	440	385654.5	3960336.0	40	87	25
2	460	385664.0	3960353.0	40	69	39
2	480	385673.5	3960370.0	40	83	50
2	500	385683.5	3960386.5	40	60	21
2	520	385694.0	3960405.0	40	65	24
2	540	385704.5	3960420.0	40	56	49
2	560	385716.0	3960438.0	40	51	45
2	580	385725.5	3960454.0	40	45	46
3	10	385414.5	3960519.5	20	48	45
3	30	385434.0	3960516.0	20	47	50
3	50	385453.0	3960509.5	20	49	48
3	70	385471.5	3960501.5	20	49	49
3	90	385490.0	3960493.0	20	49	55
3	110	385507.5	3960482.5	20	51	55
3	130	385521.5	3960469.0	20	55	54
3	150	385536.5	3960458.5	20	59	55
3	170	385555.5	3960458.0	20	57	56
3	190	385575.5	3960461.0	20	53	51
3	210	385595.0	3960460.5	20	54	54
3	230	385611.0	3960451.5	20	56	53
3	250	385623.5	3960436.0	20	57	45
3	270	385638.0	3960421.5	20	57	46
3	290	385654.5	3960409.5	20	60	54
3	310	385672.0	3960402.0	20	56	71
3	330	385691.5	3960401.0	20	53	95
3	350	385711.5	3960402.0	20	65	165
3	370	385731.5	3960400.5	20	71	270

APPENDIX B: TIME-DOMAIN SOUNDING MODELS

Fitting errors (the difference between observed time-domain decays and those that would be predicted by the model that best fits the observed decays) and the best-fit models (including layer thickness, layer conductivity, and depth to the top of each layer) for five soundings acquired at the Flowers Ranch site in May 2011. Sounding locations are shown on Fig. 1. Graphical depictions of the best-fit conductivity models are shown on Figs. 9 to 13.

Sounding	FR2 (hr1g1)		
Fitting error (%)	1.22		
Layer	**Thickness (m)**	**Conductivity (mS/m)**	**Depth at top (m)**
1	7.6	23.1	0.0
2	32.3	68.8	7.6
3	77.2	46.9	39.9
4	125.4	96.7	117.1
5	—	336.1	242.5

Sounding	FR3 (hr2g2)		
Fitting error (%)	1.84		
Layer	**Thickness (m)**	**Conductivity (mS/m)**	**Depth at top (m)**
1	24.1	46.6	0.0
2	23.3	78.1	24.1
3	56.6	32.0	47.4
4	167.3	94.3	104.1
5	—	394.8	271.3

Sounding	FR4 (hr1g1)		
Fitting error (%)	1.30		
Layer	**Thickness (m)**	**Conductivity (mS/m)**	**Depth at top (m)**
1	24.3	50.9	0.0
2	16.3	106.1	24.3
3	95.4	48.1	40.6
4	107.5	77.2	136.0
5	—	305.9	243.5

Sounding	FR5 (hr2g8)		
Fitting error (%)	1.67		
Layer	**Thickness (m)**	**Conductivity (mS/m)**	**Depth at top (m)**
1	17.8	44.0	0.0
2	18.2	93.2	17.8
3	95.1	47.5	36.0
4	144.3	88.1	131.0
5	—	255.4	275.4

Sounding	FR7 (hr2g4)		
Fitting error (%)	1.50		
Layer	**Thickness (m)**	**Conductivity (mS/m)**	**Depth at top (m)**
1	32.2	77.3	0.0
2	63.2	43.8	32.2
3	167.8	65.1	95.4
4	—	188.3	263.2